THE JOURNAL OF BIOLOGICAL CHEMISTRY
Vol. 278, No. 43, Issue of October 24, pp. 42300–42306, 2003

Printed in U.S.A.

Structure-based Incorporation of 6-Methyl-8-(2-deoxy-β-ribofuranosyl)isoxanthopteridine into the Human Telomeric Repeat DNA as a Probe for UP1 Binding and Destabilization of G-tetrad Structures*

Received for publication, June 11, 2003, and in revised form, August 5, 2003
Published, JBC Papers in Press, August 6, 2003, DOI 10.1074/jbc.M306147200

Jeffrey C. Myers, Sheila A. Moore, and Yousif Shamoo‡

From the Department of Biochemistry and Cell Biology, Rice University, Houston, Texas 77005

Heterogeneous ribonucleoprotein A1 (hnRNP A1) is an abundant nuclear protein that participates in RNA processing, alternative splicing, and chromosome maintenance. hnRNP A1 can be proteolyzed to unwinding protein (UP1), a 22.1-kDa protein that retains a high affinity for purine-rich single-stranded nucleic acids, including the human telomeric repeat (hTR) d(TTAGGG)$_n$. Using the structure of UP1 bound to hTR as a guide, we have incorporated the fluorescent guanine analog 6-MI at one of two positions within the DNA to facilitate binding studies. One is where 6-MI remains stacked with an adjacent purine, and another is where it becomes fully unstacked upon UP1 binding. The structures of both modified oligonucleotides complexed to UP1 were determined by x-ray crystallography to validate the efficacy of our design, and 6-MI has proven to be an excellent reporter molecule for single-stranded nucleic acid interactions in positions where there is a change in stacking environment upon complex formation. We have shown that UP1 affinity for d(TTAGGG)$_2$ is ~5 nM at 100 mM NaCl, pH 6.0, and our binding studies with d(TTAGG(6-MI)TTAGGG) show that binding is only modestly sensitive to salt and pH. UP1 also has a potent G-tetrad destabilizing activity that reduces the T_m of the hTR sequence d(TAGGGT)$_4$ from 67.0 °C to 36.1 °C at physiological conditions (150 mM KCl, pH 7.0). Consistent with the structures determined by x-ray crystallography, UP1 is able to bind the hTR sequence in solution as a dimer and supports a model for hnRNP A1 binding to nucleic acids in arrays that may make a contiguous set of anti-parallel single-stranded nucleic acid binding clefts. These data suggest that seemingly disparate roles for hnRNP A1 in alternative splice site selection, RNA processing, RNA transport, and chromosome maintenance reflect its ability to bind a purine-rich consensus sequence (nYAGGn) and destabilize potentially deleterious G-tetrad structures.

The eukaryotic nucleus contains an abundant family of RNA binding proteins called heterogeneous ribonucleoproteins (hnRNP).[1] Although hnRNPs were among the first eukaryotic RNA-binding proteins isolated, their role *in vivo* is complex and not fully delineated. hnRNP A1 is tightly associated with DNA polymerase II transcripts, and recent work has suggested that they may play an important role in the retention of intron-containing pre-mRNA within the nucleus (1) as well as already established roles in alternative splicing (2–10) and RNA transport (11–14). In addition, hnRNP A1 has been demonstrated to bind purine-rich DNAs such as the human telomeric repeat (hTR) d(TTAGGG)$_n$ (15–18) and mouse minisatellite (MN) repeat d(GGCAG)$_n$ (19). The observation that UP1 binds with high affinity to these repeat sequences has suggested an *in vivo* role for hnRNP A1 and its proteolytic derivative UP1 in chromosome maintenance (16, 18).

Human hnRNP A1 is a 319-amino acid protein (34 kDa) made up of three domains (20, 21). The first two-thirds of the protein contain two canonical RNA recognition motifs (RRM) that have been shown to bind tightly to ssRNA (22, 23). The C-terminal domain of hnRNP A1 is composed largely of small, highly flexible residues (40% glycine) and several RGG motifs that contribute to hnRNP A1 cooperativity and affinity for ssRNA (22, 24). The nuclear localization signal of hnRNP A1 is in the flexible C-terminal domain, as are several potential phosphorylation (25) and methylation sites that mediate hnRNP A1 localization and affinity for ssRNA (26). Partial proteolysis studies of hnRNP A1 showed that the C-terminal 124 residues could be removed readily to produce UP1. UP1 is made up of residues 1–195 and includes both RRMs as well as a short basic region just C-terminal of RRM2 that is important to nucleic acid binding (23). Unlike most RRM-containing proteins, UP1 is able to bind with high affinity to either ssDNA or ssRNA (22, 23, 27).

The structure of UP1 has been determined alone (28, 29) and with the short telomeric DNA sequence d(TTAGGG)$_2$ (30). The arrangement of protomers in the crystal structures showed that the nucleic acid binding groove of UP1 is made by two copies of UP1 that bind ssDNA such that the two DNA strands bind in an anti-parallel fashion (Fig. 1). The ssDNA in the crystal structure of Ding *et al.* (30) has an extended conforma-

* This work was supported by a fellowship from The Welch Foundation (to J. M.) and National Institutes of Health Grant RO3 HD39658-2 (to Y. S.). The costs of publication of this article were defrayed in part by the payment of page charges. This article must therefore be hereby marked "*advertisement*" in accordance with 18 U.S.C. Section 1734 solely to indicate this fact.

The atomic coordinates and structure factors (codes 1PO6, 1PGZ, and 2UP1) have been deposited in the Protein Data Bank, Research Collaboratory for Structural Bioinformatics, Rutgers University, New Brunswick, NJ (http://www.rcsb.org/).

‡ To whom correspondence should be addressed: Dept. of Biochemistry and Cell Biology, Rice University, MS-140, 6100 S. Main St., Houston, TX 77005. Tel.: 713-348-5493; Fax: 713-348-5154; E-mail: Shamoo@rice.edu.

[1] The abbreviations used are: hnRNP, heterogeneous ribonucleoprotein; hTR, human telomeric repeat; MN, minisatellite; RRM, RNA recognition motif; UP1, unwinding protein 1 (residues 1–195 of hnRNP A1); 6-MI, 6-methyl-8-(2-deoxy-β-ribofuranosyl)isoxanthopteridine; ssRNA, single-stranded RNA; ssDNA, single-stranded DNA; SELEX, systematic evolution of ligands by exponential enrichments; BSA, bovine serum albumin; Y, pyrimidine; TR2, d(TTAGGG)$_2$; MES, 4-morpholineethanesulfonic acid.

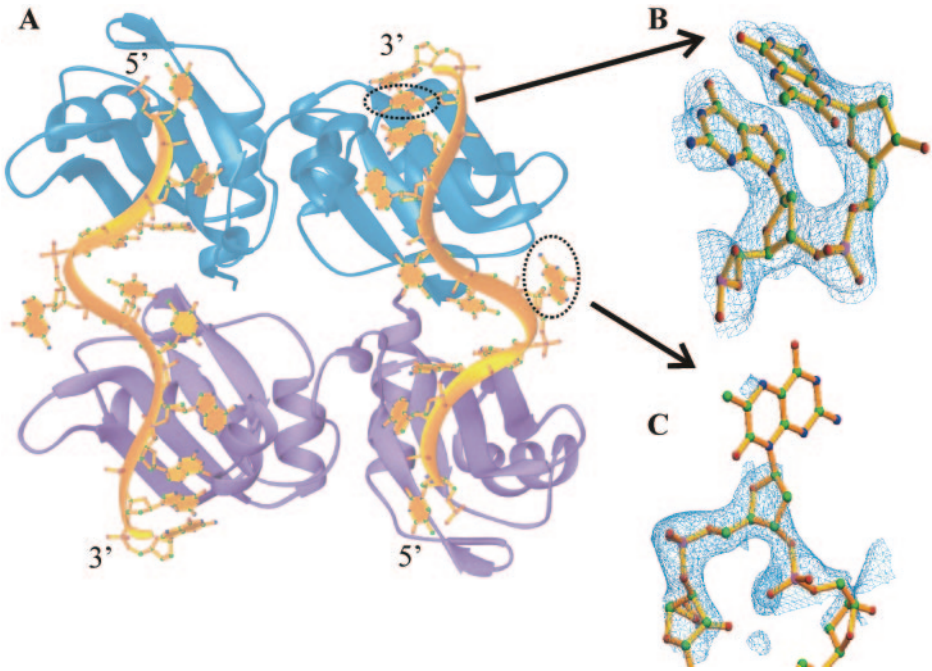

FIG. 1. *A*, ribbons diagram (50) of UP1 bound to the sequence d(TTAGGGTTAGGG). Two copies of UP1 form a crystallographic dimer in which the DNA is bound in an anti-parallel arrangement across RRM1 (residues 1–92) and RRM2 (residues 93–195) from the two UP1 molecules. The 2-fold rotation of the UP1 molecules into the crystallographic dimer permits the formation of a contiguous single-stranded nucleic acid binding cleft. Previous studies have shown that UP1 has an RNA binding site size of 15 nucleotides, which is in good agreement with the structure. The positions of the 6-MI substitutions in oligonucleotides TR2-6F and TR2-11F are indicated (*circles*). *B*, $2F_o - F_c$ electron density from a composite omit map of 6-MI substituted for Gua-11 (TR2-11F) contoured at 1.2 σ. *C*, electron density of 6-MI from a $2F_o - F_c$ composite omit map generated using phases obtained from molecular replacement of UP1 bound to d(TTAGGGTTAGGG) contoured at 1.2 σ. The model shows the position of 6-MI in TR2-6F (*blue*). The electron density corresponding to the phosphodiester and deoxyribose atoms at position six are of good quality, whereas the highly mobile base appears only weakly. This finding is consistent with electron density maps derived from the wild-type structure that was resolved in our laboratory for comparison. In both the original and substituted DNA, the base at position 11 stacks with Gua-10 and makes interactions through the base O6 (O4 in 6-MI) to the main chain of UP1. In contrast to TR2-6F, the electron density of 6-MI in TR2-11F is moderately well ordered.

tion (average interatomic phosphate distance of 6.6 Å) with each RRM making a network of stacking, hydrogen bonding, hydrophobic, van der Waals, and electrostatic interactions to about four nucleotides in excellent agreement with prior estimates of DNA-binding site size based on polynucleotide binding studies (23). Although the crystal structures indicate an extended DNA conformation upon UP1 binding, it has been shown that hTR sequences form stable quadruplex structures under a wide range of solution conditions (31, 32), and we have shown, consistent with the work of Fukuda *et al.* (19), that UP1 destabilizes G-tetrad structures *in vitro*, an activity that may provide an important clue for the *in vivo* activities of hnRNP A1.

We have used the available high resolution structures of UP1 to incorporate the fluorescent guanosine analog 6-methyl-8-(2-deoxy-β-ribofuranosyl)isoxanthopteridine (6-MI) into the oligonucleotide $d(TTAGGG)_2$ as a probe for studying UP1 interactions to hTR DNA (33, 34). Previous fluorescence studies using either the quenching of intrinsic tryptophan fluorescence or the fluorescent nucleotide riboethanoadenylic acid have shown that UP1 binds promiscuously to single-stranded nucleic acids as part of its *in vivo* role in RNA processing and transport (22, 23, 27). SELEX experiments originally identified UAGGG(A/U) repeats as potential high affinity sites for hnRNP A1 (9). More recent work using gel mobility shift assays and surface plasmon resonance imaging have shown that UP1 and intact hnRNP A1 bind with high affinity to hTR sequences (19). Incorporation of 6-MI into hTR sequences as a reporter for UP1 binding has allowed us to perform equilibrium binding studies and evaluate the utility of 6-MI as a potential probe for other protein/single-strand nucleic acid interactions. The available structure and prior characterization of UP1 as a prototypical ssRNA binding protein provide an excellent framework for these studies.

Although crystallographic studies indicate that UP1 may bind as a dimer to single-stranded nucleic acids, previous solution studies have not supported such a model. hnRNP A1, but not UP1, has been shown to have a modest cooperativity upon binding to RNA polynucleotides. By using light scattering, we have shown that UP1 is able to specifically bind hTR sequences as a dimer, but only in the presence of a sufficiently long single-stranded nucleic acid. Taken together, our equilibrium binding studies, light scattering, x-ray studies, and DNA melting experiments support a model for hnRNP A1 activity that includes the destabilization of adventitious G-tetrad-stabilized quadruplexes using a preference for purine-rich (nYAGGn) sequences.

MATERIALS AND METHODS

Purification of UP1—Plasmid pYS45 was used for the overexpression of UP1 in *Escherichia coli* BL21(DE3), and purification of UP1 was based upon Shamoo *et al.* (23) with some modifications. Cells were disrupted by sonication, and the crude cell lysate was passed over a DE52 anion exchange column (UP1 flows through) and an ssDNA cellulose column connected in series that had been equilibrated in buffer A (10 mM Tris, pH 8.0, 50 mM NaCl, 0.1 mM EDTA, 0.1 mM phenylmethylsulfonyl fluoride, 1 mM dithiothreitol, and 10% glycerol (v/v)). UP1 was eluted from the ssDNA cellulose column with a step gradient using buffer A + 1.0 M NaCl and dialyzed into Buffer B (20 mM MES, pH 6.0, 35 mM NaCl, 1 mM EDTA, 1 mM dithiothreitol, and 10% glycerol (v/v)). UP1 was then bound to a HiTrap heparin affinity column (Amersham Biosciences) and eluted by using a linear gradient from 0.035 to 1.0 M NaCl. UP1 was again dialyzed against buffer B and then passed over a HiTrap Sepharose SP FF cation exchange column (Amersham Biosciences) and eluted with a gradient extending to 1.0 M NaCl. Purified UP1 was dialyzed against 20 mM MES, pH 6.0, 300 mM NaCl, 1 mM EDTA, and 0.1% β-mercaptoethanol (v/v) and concentrated to 40

mg/ml using a 10,000 molecular weight cutoff concentrator (Vivaspin 20, Vivascience) and then flash frozen in liquid nitrogen.

Oligonucleotides—All oligonucleotides (TR2-6F, d(TTAGG(6-MI)TTAGGG); TR2-11F, d(TTAGGGTTAG(6-MI)G) were obtained commercially (IDT, MWG Biotech Inc., and TriLink Biotechnologies for 6-MI) and purified by high pressure liquid chromatography on a Vydac C4 reverse phase column.

Crystallization of the UP1·TR2-6F and UP1·TR2-11F Complexes—Crystals were grown with the vapor diffusion method at 10 °C at an initial starting UP1 concentration of 0.83 mM. 1.5 μl of UP1·TR2-6F (1:1.5 stoichiometry) was incubated on ice for 1.5 h prior to being mixed with 2.5–3.75 μl of precipitant. The precipitant contained 100 mM Tris, pH 8.5, 15% glycerol (v/v), and 1.8–2.2 M dibasic ammonium phosphate. Crystals took 3–5 days to grow.

Data Collection and Structure Solution—UP1·TR2-6F and UP1·TR2-11F diffraction data were collected on a Rigaku R-Axis IV^{++} detector with Osmic mirrors at −170 °C. Both crystals grew in space group $P4_32_12$ with unit cell dimensions $a = b = 51.8$ Å, $c = 172.3$ Å (TR2-6F), and $a = b = 51.6$ Å, $c = 171.5$ Å (TR2-11F), with two copies of UP1 per asymmetric unit. For TR2-6F, reflections were 96% complete to 2.1 Å and had an average I/σ = 2.4 in the highest resolution bin (2.09–2.05 Å) and an overall redundancy of 3.9. For TR2-11F, reflections were 95% complete to 2.6 Å and had an average I/σ = 4.4 in the highest resolution bin (2.64–2.60 Å) and an overall redundancy of 5.4. Diffraction data were collected using CrystalClear (Rigaku/MSC) and processed with DENZO, and intensities were scaled with SCALEPACK (35). The structures were solved with Crystallography NMR System by molecular replacement using the structure of Ding *et al.* (30) (2UP1) as a search model (36). 6-MI was built starting from an energy-minimized structure (37, 38) and parameterized for Crystallography NMR System using the software XPLO2D (38). The final models fit the data, with $R_{calc} = 0.23$ and $R_{free} = 0.26$ for TR2-6F (1PO6) and $R_{calc} = 0.24$ and $R_{free} = 0.27$ for TR2-11F (1PGZ).

Equilibrium Fluorescence Titrations—Equilibrium binding experiments were performed with an SLM 8100 spectrometer (SLM Instruments) as a "forward titration" by titrating UP1 into a cuvette containing oligonucleotides incorporating 6-MI and measuring the gain of signal as a function of complex formation (39). An excitation wavelength of 340 nm and emission of 430 nm was used at 25 °C with 1-cm path length cuvettes (33). Ten measurements were taken 450 s after each addition of UP1, and the average was taken as one data point. A control of oligonucleotide alone was also used to correct for changes in the detector base-line and photobleaching. For titrations with varying NaCl concentrations, TR2-6F concentration was 250 nM in 20 mM MES, pH 6.0, and 4-nm band-passes were used for both the excitation and emission monochromators without polarizers. Competition binding experiments were performed at 0.5 μM TR2-6F in 100 mM NaCl and 20 mM MES, pH 6.0. Titrations with variable pH used 10 nM TR2-6F in 20 mM MES (pH 6.0, 6.5) or 20 mM HEPES (pH 7.0, 7.5, 8.0) in 300 mM NaCl, and 8-nm band-passes were used for both monochromators. Titration curves were fitted using Dynafit (BioKin Ltd., Pullman, WA).

Thermal Denaturation of Quadruplex Nucleic Acids—Melting assays were performed in either 150 mM KCl, 10 mM potassium cacodylate, pH 7.0, or 100 mM KCl, 10 mM potassium cacodylate, pH 6.5. Experiments were carried out with 3 μM d(TAGGT)$_4$, 3 μM mouse MN d(GGCAG)$_4$, and 6 μM UP1. The melting assays were run on a Lambda 20 UV-visible spectrometer (PerkinElmer Life Sciences) that included a Peltier model PTP-6 temperature controller. All melting data were collected at 295 nm as a function of temperature over the range of 5–85 °C, with a fixed heating rate of 1.0 °C/min. Prior to melting, the DNA was incubated at 85 °C for 5 min and then allowed to anneal to room temperature. For the protein/DNA complexes, the annealed DNA was chilled on ice before UP1 was added. For data collected at temperatures less than 20 °C, the chamber of the spectrometer was sparged with nitrogen to reduce humidity.

Static Light Scattering—A miniDAWN three-angle light-scattering photometer (Wyatt Technology, Santa Barbara, CA) was used to determine the molecular weight of individual proteins and complexes. 150–300-μg samples were injected onto a Shodex KW803 gel filtration column at a flow rate of 0.5 ml/min, and their elution was monitored by Shimadzu SPD-10Avp UV-visible and Waters R401 refractive index detectors. All measurements were made in 0.1 M KCl, 10 mM potassium cacodylate (pH 6.5) at 20 °C. The miniDAWN was calibrated according to the manufacturer's instructions (Wyatt Technology), and BSA was used as a standard to evaluate the accuracy of the system. A *dn/dc* value of 0.184 was used for BSA and single proteins (40). *dn/dc* values for complexes were determined by using both UV-visible detector (280 nm) and differential refractometer. UV calibration constants used were calculated from the known extinction coefficients of the components and confirmed empirically by using their absorbance at 280 nm. The Zimm method was used to determine the molecular masses for all samples (41).

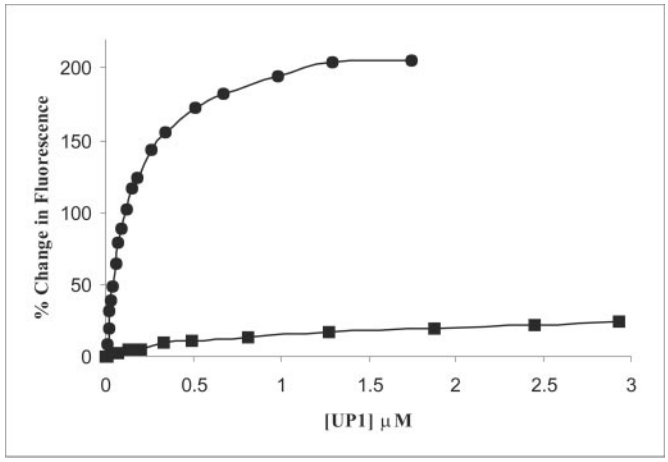

FIG. 2. **Fluorescence titration of UP1 with TR2-6F (●) and TR2-11F (■).** Fluorescent signal of 6-MI is strongly influenced by its environment. In TR2-6F, 6-MI becomes fully unstacked and solvent-exposed upon UP1 binding. In TR2-11F, 6-MI stacks with neighboring Gua-10 when bound to UP1. Excitation and emission wavelengths were 340 and 430 nm, respectively, and both titrations were performed in 20 mM MES, pH 6.0, and 100 mM NaCl at 25 °C. Total gain-of-signal for TR2-6F was 3.3× the base-line; for TR2-11F, it was 1.2× base-line.

RESULTS

Structure of UP1 Complexed to TR2-6F and TR2-11F—X-ray diffraction analysis was used to determine the structure of UP1 bound to oligonucleotides incorporating 6-MI. The UP1·TR2-6F co-crystals diffracted to 2.1 Å, and composite omit maps of the region around the sixth position clearly indicated that substitution of 6-MI for guanine had no significant effect on the overall structure. A least squares superposition of Cαs from the structures of UP1 bound to TR2-6F and TR2 (d(TTAGGG)$_2$) showed no significant differences (root mean square deviation = 0.23 Å). Electron density for the fully refined structure of UP1 bound to TR2-6F showed only very weak density (Fig. 1*B*) for 6-MI at position 6 and is consistent with high mobility resulting from complete destacking upon complex formation. The wild-type structure showed comparably weak electron density for Gua-6, which further supports the conclusion that positioning of 6-MI led to no substantive changes in the co-structure.

The substitution of Gua-11 with 6-MI was also determined and compared with the wild-type structure (Fig. 1*C*). Unlike the Gua-6 substitution, Gua-11 makes a hydrogen bond through the O-6 position to a main chain amide and is proximal to the aliphatic portion of the side chain for Lys-183. The UP1·TR2-11F co-crystals were small and diffracted to 2.6 Å on a conventional rotating anode source. The overall root mean square deviation from the superposition of the wild-type and TR2-11F Cαs was 0.29 Å, suggesting that there were no larger global changes to the complex structure upon substitution of 6-MI at position 11. We observed that the structure of TR2-11F bound to UP1 shows that Gua-12 is disordered, whereas in the native structure, Gua-12 stacks with Gua-11. However, inspection of the native structure suggests that there are no direct contacts between Gua-12 and UP1.

6-MI Gain-of-signal Depends Strongly upon Change of Environment during Complex Formation—Fig. 2 shows the fluorescence emission spectra of TR2-6F and TR2-11F at a concentration of 10 nM during UP1 binding. TR2-6F shows a 3- to 4-fold increase in fluorescence emission at 430 nm upon complex

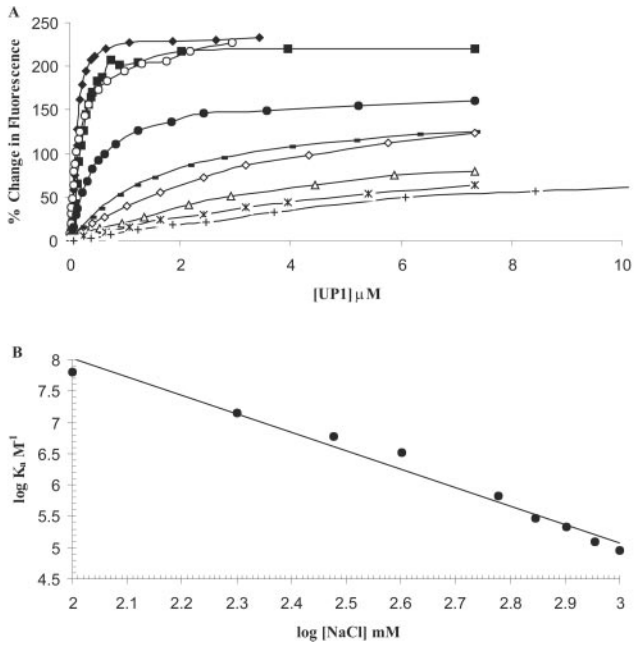

FIG. 3. *A*, fluorescence titrations of UP1 with TR2-6F at different concentrations of NaCl. All measurements were performed in 20 mM MES, pH 6.0, at 0.1 M NaCl (♦), 0.2 M NaCl (■), 0.3 M NaCl (○), 0.4 M NaCl (●), 0.6 M NaCl (■), 0.7 M NaCl (◇), 0.8 M NaCl (△), 0.9 M NaCl (*), and 1.0 M NaCl (+). *B*, log K_a of the above titrations *versus* log [NaCl] mM. Data were fitted by a linear least squares fit, and they produced a slope of −2.9 and a *y* intercept of 14 (note that *x*-axis does not begin at zero). The number of ionic interactions was estimated to be ~4 and was determined by dividing the slope by the thermodynamic constant for the fraction of counter-ions bound per phosphate for ssDNA ($\psi = 0.71$) (47), as described by Mascotti and Lohman (43).

formation, whereas TR2-11F shows only a modest 1.2-fold increase in intensity. The differences in magnitude of the changes in intensity for the TR2-6F and TR2-11F are consistent with their structures when bound to UP1, in which 6-MI in TR2-6F is completely solvent-accessible and 6-MI in TR2-11F remains stacked with Gua-10.

Fluorescence Binding Studies of UP1 to TR2-6F and TR2-11F—Estimates of equilibrium dissociation rates were made for both oligonucleotides by using a forward titration of 10 nM TR2-6F and TR2-11F with increasing amounts of UP1 (Fig. 2). Binding isotherms were fitted to the data ("Materials and Methods") and displayed stoichiometric binding to TR2-6F (~50 nM) at salt concentrations approximating those found *in vivo* (100–200 mM). To determine accurate dissociation constants, it was necessary to evaluate binding as a function of salt concentration and pH.

Fluorescence Binding Studies of UP1 to TR2-6F as a Function of Salt Concentration and pH—Fig. 3*A* shows the binding of UP1 to TR2-6F as a function of NaCl concentration from 0.1 to 1.0 M (Table I). The binding of UP1 is moderately sensitive to salt concentration and is consistent with its role in both specific and non-sequence-specific binding of single-stranded nucleic acids. The slope of the log K_a *versus* log salt (NaCl) concentration (Fig. 3*B*) was used to estimate the electrostatic contribution for TR2-6F binding to UP1 (42, 43). A slope of −2.9 is in good agreement with UP1 binding to ssRNA, although the overall binding to TR2-6F is 1000-fold stronger than the values measured for poly ribo-ethanylated RNA and poly uracil (22, 23).

Fig. 4 shows that pH has little effect on UP1·TR2-6F complex formation over a range of pH (6.0–7.5), and only an 8% reduction in K_d was observed over this range. A 2-fold decrease in binding was observed between pH 7.5 and pH 8.0 (Table II).

TABLE I
Dissociation constants measured for UP1 binding to TR2-6F at increasing concentrations of NaCl

[NaCl]	K_d
mM	*μM*
100	0.016
200	0.071
300	0.166
400	0.299
600	1.51
700	3.44
800	4.76
900	7.89
1000	11.3

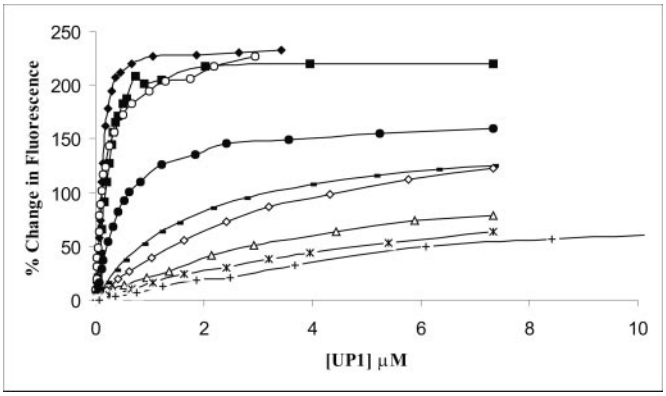

FIG. 4. **Fluorescence titrations of UP1 with TR2-6F at various pHs.** All measurements were performed at 0.3 M NaCl with 20 mM MES (pH 6.0, pH 6.5) or 20 mM HEPES (7.0–8.0). ♦, pH 6.0; ■, pH 6.5; ▲, pH 7.0; ●, pH 7.5; ○, pH 8.0.

TABLE II
Dissociation constants measured for UP1 binding to TR2-6F as a function of pH

pH	K_d
	nM
6.0	145
6.5	118
7.0	157
7.5	158
8.0	321

Thermal Denaturation of Telomeric d(TTAGGG)$_4$ and MN d(GGCAG)$_5$ Repeats by UP1—Destabilization of nucleic acid structures by proteins can be readily monitored as a reduction of the nucleic acid melting temperature (T_m) (44). Both hnRNP A1 and UP1 are able to reduce the T_m of the poly[r(A-U)] and [d(A-T)] by having a much greater affinity for single-stranded compared with double-stranded nucleic acid. Fukuda *et al.* (19) have shown that UP1 destabilizes the mouse MN repeat and variations of that sequence. We have also found that UP1 is able to strongly destabilize the G-tetrad-stabilized quadruplex structures found in both human telomeric d(TAGGGT)$_4$ and mouse MN d(GGCAG)$_5$. Both the hTR and MN DNA quadruplexes have characteristic hypochromic shifts at 295 nm, and we have used the depression of this signature signal to monitor UP1 binding and subsequent destabilization of the quadruplex structures (32, 45). As shown in Fig. 5, UP1 reduces the T_m of d(TAGGGT)$_4$ from 67.0 to 36.1 °C at 150 mM KCl, pH 7.0 and that of d(GGCAG)$_5$ from 56.0 to 17.8 °C at 100 mM KCl, pH 6.5. We were unable to measure a T_m for the interaction of UP1 to d(GGCAG)$_5$ at the more physiological 150 mM KCl concentration because melting was occurring prior to the start of the experiment at 5 °C (not shown). The melting data are consistent with recent circular dichroism studies that indicated UP1 is

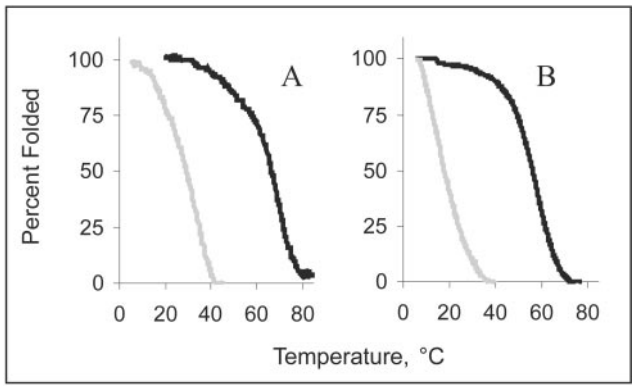

FIG. 5. **Thermal denaturation of G-tetrad-forming DNA by UP1.** Normalized melting profiles at 295 nm of hTR4 = $d(TAGGGT)_4$ and mouse MN4 = $(GGCAG)_5$ alone and in the presence of UP1. Destabilization of G-tetrad-stabilized quadruplexes is determined by the change in the T_m (T_m = 50% of the hypochromic shift). *A*, 3 μM hTR4 (*black*), 3 μM hTR4 + 6 μM UP1 (*gray*) in 150 mM KCl, and 10 mM potassium cacodylate, pH 7.0. *B*, 3 μM mouse MN4 (*black*), 3 μM mouse MN4 + 6 μM UP1 (*gray*) in 100 mM KCl, and 10 mM potassium cacodylate, pH 6.5.

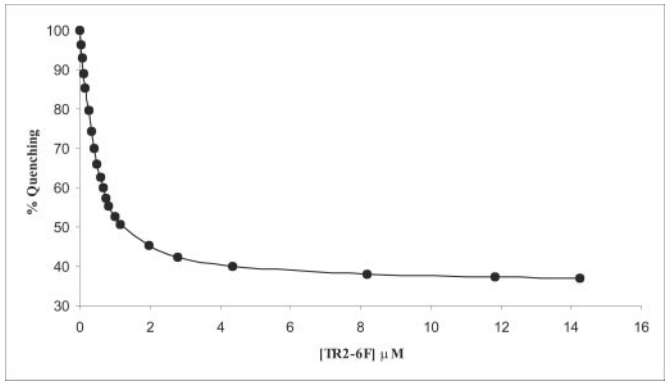

FIG. 6. **Competition binding of TR2 *versus* TR2-6F.** TR2 was titrated into a cuvette containing 0.5 μM UP1 and 0.5 μM TR2-6F in 100 mM NaCl and 20 mM MES, pH 6.0. A loss-of-signal was observed, and data were fit by using Dynafit (BioKin Ltd.), yielding a K_d = 6.5 nM.

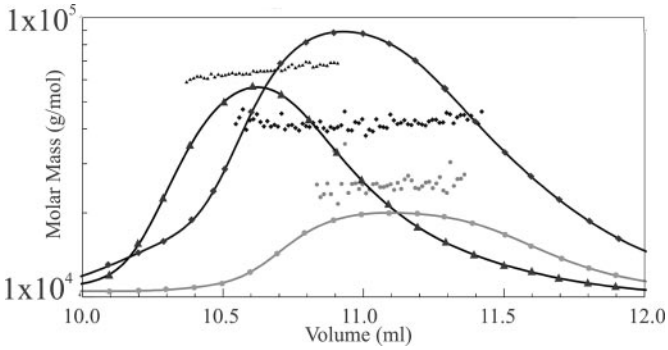

FIG. 7. **Light scattering studies of UP1 complexed to $d(TTAGGG)_2$.** Molecular mass is indicated for: ▲, 9 μM BSA (calculated mass = 66.4 kDa); ●, 9 μM UP1 (calculated mass = 22.1 kDa); ♦ 9 μM UP1 + 9 μM $d(TTAGGG)_2$ (calculated monomer mass = 25.9 kDa, dimer = 51.8 kDa) in 100 mM KCl and 10 mM potassium cacodylate (pH 6.5) at 20 °C. The chromatographic peaks represent absorbance at 280 nm from the elution of the gel filtration column, and the points represent the weight-averaged molecular masses across the peak for each species tested.

able to induce changes in the ellipticity of these repeat sequences (19). Similar studies performed with $d(TTAGGG)_2$ and $r(TTAGGG)_2$ also showed a reduced T_m but could not be quantitated because the melting began prior to the starting temperature (5 °C). Substitution of the guanine analog 6-MI for either the 6th or 11th guanine in $d(TTAGGG)_2$ showed that 6-MI did not support G-tetrad formation (not shown).

Competition Binding Studies—In light of our findings that TR2-6F and TR2-11F did not support G-tetrad formation, we measured the affinity of UP1 for the sequence $d(TTAGGG)_2$ in a competition binding assay (Fig. 6). The stable G-tetrad structure observed for the hTR and MN DNA by thermal denaturation studies would presumably have to be denatured by UP1 to form the extended structure seen in the crystallographic studies. The binding of $d(TTAGGG)_2$ at 100 mM NaCl was found to be ~5 nM at pH 6.0.

Light Scattering Suggests UP1 Is Able to Bind as a Dimer to Nucleic Acids—The molecular mass of UP1 and UP1 complexed to hTR DNAs was determined by light scattering under conditions similar to those used in the fluorescence, thermal denaturation, and x-ray crystallography studies. UP1 alone was found to be monomeric with a mass of 23.5 kDa, which was within 5% of the calculated mass and in good agreement with the accuracy obtained from our known protein standard, BSA. Fig. 7 shows the weight-averaged molecular mass across the chromatographic peaks for UP1 and UP1 bound to $d(TTAGGG)_2$. The UP1·$d(TTAGGG)_2$ complex had a mass of 41.9 kDa and was 19.1% lower than the expected dimer mass, assuming two copies of UP1 and of the DNA. No other chromatographic peaks at 280 or 260 nm were observed in the elution profile, suggesting that the low estimate is the result of an error in the calculation of *dn/dc* and the UV calibration constant for the protein·nucleic acid complex. A similar underestimate was observed for the mass of DNA polymerase·primer-template complexes (40). UP1 alone was somewhat polydispersed at the solution conditions used in these experiments (0.1 M KCl, 10 mM potassium cacodylate, pH 6.5).

DISCUSSION

We have shown that the proper positioning of 6-MI as a reporter can be highly effective for structure-function studies when there is a high resolution structure available. Based upon previous studies suggesting that 6-MI is an excellent fluorescent guanosine analog in duplex DNA, we synthesized two singly substituted oligonucleotides with two hTR repeats, TR2-6F and TR2-11F. Unlike double-stranded DNA-binding proteins, single-stranded nucleic acid-binding proteins can use nearly all the sugar-phosphate backbone and base positions for specificity, and, therefore, some care is necessary for using modified nucleotides (46). 6-MI closely resembles guanine (Fig. 1*B*) and has a position analogous to N7, but the presence of a methyl group at the pteridine C3 would make this position less accessible. Other steric and electrostatic differences induced by the methyl and carbonyl groups at positions three and two, respectively, could undermine sequence-specific protein/ssDNA interactions such that its utility may be limited. This consideration prompted us to use the UP1-hTR structure as a guide for positioning 6-MI as a reporter for binding.

Using the program ENTANGLE to inspect the UP1-hTR co-structure, we found that the guanine base at position 6 makes no direct contacts with UP1 and is solvent accessible upon complex formation (46). The substitution of Gua-11 with 6-MI was also chosen to test the utility of 6-MI as a probe for binding in those cases where the fluorescent base remains stacked upon binding. As before, 6-MI was substituted at a position where interactions with UP1 are limited, although in this case the Gua-11 makes a hydrogen bond to the main chain amide of Lys-183 and stacks between Gua-10 and Gua-12. In either case, no substantive changes were seen in the crystal structures of the 6-MI-substituted oligonucleotides bound to UP1 compared with wild type, suggesting that we were suc-

cessful in an innocuous placement of the modified nucleosides.

The oligonucleotides TR2-6F and TR2-11F were then evaluated as reporters for UP1·hTR complex formation by exciting at 340 nm and measuring the gain-of-signal at 430 nm. The two positions represent different approaches to employing 6-MI. The first substitution at position 6 was chosen on the assumption that the purine-rich hTR remains partially stacked as a single-stranded oligonucleotide. DNA melting studies have shown that incorporation of 6-MI at either the 6 or 11 position abrogate quadruplex formation under the solution conditions for our binding studies. This finding is not surprising, considering the strict geometry of quadruplexes and the fact that the analogous N7 of 6-MI would not be positioned properly. The gain-of-signal seen in Fig. 2 is consistent with the unstacking of bases upon complex formation, and its strength permitted us to decrease the concentration of TR2-6F to 10 nM and obtain binding isotherms under tight binding conditions. This is in marked contrast to either intrinsic tryptophan fluorescence of UP1 or ribo-ethanylated RNA that requires micromolar quantities of reporter, thus limiting the ability to measure binding of UP1 to high affinity targets such as the hTR.

The strength of UP1 binding to hTR sequences is consistent with a physiologically relevant role for hnRNP A1/UP1 in binding available purine-rich sequences (nYAGGn) found in consensus splice sites, hTR and MN sequences. UP1 binds stoichiometrically to $d(TTAGGG)_2$ with an estimated K_d of ~5 nM in 100 mM NaCl at pH 6.0. UP1 binding is only moderately sensitive to salt and pH (Tables I and II), and electrostatic contributions make up ~15% of the overall affinity of UP1 for hTR DNA and is similar to that measured for non-sequence-specific UP1 binding to polynucleotides. Record *et al.* (47) have shown that the number of ionic interactions is correlated to the slope of data fitted to a log K_a *versus* log [NaCl] plot. In the case of UP1, the number of interactions predicted is ~4, and the crystal structure shows that Arg-55, Arg-92, Arg-140, and Arg-146 are within 5 Å of phosphodiester oxygen atoms. Because one proposed role for hnRNP A1 *in vivo* is the generalized transport of mature DNA polymerase II mRNAs, these data suggest that the transport of mRNA may proceed through non-specific and largely electrostatic interactions, whereas the high affinity association of UP1 and hnRNP A1 to purine-rich sequences containing the consensus sequence (nYAGGn) will be dominated by hydrogen bonding, stacking, and hydrophobic interactions, as seen in the crystal structure.

Fukuda *et al.* (19) have shown that UP1 is able to unfold unimolecular quadruplex DNA derived from mouse MN repeats from the sequence $d(GGCAG)_n$ *in vitro*. Our own melting studies confirm these findings with this sequence as well as with the hTR repeat and shed light on a possible consensus binding sequence. hnRNP A1 and UP1 can destabilize quadruplex structures by binding to available single-stranded nucleic acid and, thereby, shift the equilibria. Single-stranded DNA-binding proteins use a similar mechanism for removing secondary structures during DNA replication, and this fact suggests UP1 may function in an analogous manner to prevent G-tetrad-stabilized quadruplexes.

Telomerase activity is found in 80–85% of proliferating tumor cells (48), and down-regulating A1 production in a mouse erythroleukemic cell line leads to shortening of telomeres (17). Direct involvement of hnRNP A1/UP1 with hTR and telomerase has been suggested (18), although our data would also support a more indirect role for hnRNP A1/UP1 in telomeric maintenance by destabilization of quadruplex structures. Presumably the removal of such quadruplex structures would aid in telomerase processivity and fidelity much as single-stranded DNA-binding proteins aid in DNA replication.

The structure of UP1 complexed with TR2 determined by Ding *et al.* (30) and our own structure studies indicate that a likely consensus binding sequence is (nYAGGn). In the crystal structure, Thy-1 of the repeat is highly disordered and does not bind with RRM1 and is not included in the crystallographic model. ENTANGLE shows that Thy-7 (the first thymine in the second repeat) also does not interact with RRM2, although it is stabilized by a stacking interaction with Arg-92, which also stacks with Gua-4. The crystal structure shows that Thy-2 and Thy-8 could potentially be replaced with cytosine as it is in mouse MN repeats. In both cases, the O2 position, nonvariant in uracil, thymine, or cytosine, accepts a hydrogen bond from a side chain amide (Lys-87 in Thy-2 and Arg-178 in Thy-8). Thus, it appears that the Thy-2 and Thy-8 binding sites on UP1 might be nonspecific among pyrimidines but discriminate against purines.

Multiple interactions occur between the RRMs of UP1 and the next three bases, AGG. In addition to its presence in hTR and mouse MNs, this repeat is found in the SELEX "winner" sequence (9) and the 5′ and 3′ distal splice site consensus sequence to which the full-length protein, hnRNP A1, has been suggested to bind in its role in pre-mRNA packaging, splicing, and transport (27). Both RRMs provide multiple stacking interactions using phenylalanine, arginine, and additional protein side and main chain interactions for base specificity. The final base in the hTR sequence corresponds to Gua-6 and Gua-12 in the crystal structure, and neither of the two interact with UP1. The solvent-exposed nature of the Gua-6 position is precisely why it was chosen for the placement of 6-MI, and Gua-12 makes no direct contact with UP1.

We have shown that the proper positioning of 6-MI in place of guanine can be an effective means of obtaining equilibrium binding data in protein·nucleic acid interactions when a structure is available, and 6-MI will prove useful in future competition experiments with UP1 and various oligonucleotides. It is important to note that 6-MI is not a perfect replacement for guanine in all situations and that it did abrogate the formation of quadruplexes in our studies.

We have also shown that UP1 dimerizes in solution in the presence of hTRs, which is consistent with the crystal structure where two copies of UP1 bind to two hTRs in an anti-parallel fashion, and that UP1 has the ability to disrupt quadruplex structures formed by native hTRs. This mode of binding may reflect the way in which hnRNP A1 associates with RNA in the context of the hnRNP complex. hnRNP A1 will bind with high affinity to any contiguous (nYAGGn) repeats, a function that may have important implications for alternative splicing. Nasim *et al.* (49) have shown that positioning high affinity hnRNP A1 binding sites to promote loop formation within pre-mRNAs can attenuate splice site selection. The binding of nucleic acid to UP1 in an anti-parallel fashion (Fig. 1) is consistent with this role in alternative splicing. One of the most puzzling attributes of hnRNP A1 is its involvement in such a wide range of *in vivo* activities, including alternative splice-site selection, RNA transport, and, most recently, in binding to mouse MN and hTR repeats. Our data suggest that highly abundant hnRNP A1 may have a broad activity in preventing the formation of G-tetrad structures that may adversely affect this diverse set of *in vivo* activities. A combination of crystallographic and physicochemical studies support the idea that UP1 binds strongly to the six-nucleotide consensus sequence (nYAGGn), which is consistent with its *in vivo* function.

Acknowledgments—We thank Drs. S. Singleton and A. Roca for bringing 6-MI to our attention.

REFERENCES

1. Reed, R., and Hurt, E. (2002) *Cell* **108,** 523–531
2. Marchand, V., Mereau, A., Jacquenet, S., Thomas, D., Mougin, A., Gattoni, R., Stevenin, J., and Branlant, C. (2002) *J. Mol. Biol.* **323,** 629–652
3. Dreyfuss, G., Kim, V. N., and Kataoka, N. (2002) *Nat. Rev. Mol. Cell. Biol.* **3,** 195–205
4. Zhu, J., Mayeda, A., and Krainer, A. R. (2001) *Mol. Cell.* **8,** 1351–1361
5. Simard, M. J., and Chabot, B. (2000) *Mol. Cell. Biol.* **20,** 7353–7362
6. Blanchette, M., and Chabot, B. (1999) *EMBO J.* **18,** 1939–1952
7. Blanchette, M., and Chabot, B. (1997) *RNA* (*N. Y.*) **3,** 405–419
8. Mayeda, A., and Krainer, A. R. (1992) *Cell* **68,** 365–375
9. Burd, C. G., and Dreyfuss, G. (1994) *EMBO J.* **13,** 1197–1204
10. Hutchison, S., LeBel, C., Blanchette, M., and Chabot, B. (2002) *J. Biol. Chem.* **277,** 29745–29752
11. Visa, N., Alzhanova-Ericsson, A. T., Sun, X., Kiseleva, E., Bjorkroth, B., Wurtz, T., and Daneholt, B. (1996) *Cell* **84,** 253–264
12. Gallouzi, I. E., and Steitz, J. A. (2001) *Science* **294,** 1895–1901
13. Pollard, V. W., Michael, W. M., Nakielny, S., Siomi, M. C., Wang, F., and Dreyfuss, G. (1996) *Cell* **86,** 985–994
14. Izaurralde, E., Jarmolowski, A., Beisel, C., Mattaj, I. W., Dreyfuss, G., and Fischer, U. (1997) *J. Cell. Biol.* **137,** 27–35
15. Ishikawa, F., Matunis, M. J., Dreyfuss, G., and Cech, T. R. (1993) *Mol. Cell. Biol.* **13,** 4301–4310
16. Dallaire, F., Dupuis, S., Fiset, S., and Chabot, B. (2000) *J. Biol. Chem.* **275,** 14509–14516
17. LaBranche, H., Dupuis, S., Ben-David, Y., Bani, M. R., Wellinger, R. J., and Chabot, B. (1998) *Nat. Genet.* **19,** 199–202
18. Fiset, S., and Chabot, B. (2001) *Nucleic Acids Res.* **29,** 2268–2275
19. Fukuda, H., Katahira, M., Tsuchiya, N., Enokizono, Y., Sugimura, T., Nagao, M., and Nakagama, H. (2002) *Proc. Natl. Acad. Sci. U. S. A.* **99,** 12685–12690
20. Cobianchi, F., SenGupta, D. N., Zmudzka, B. Z., and Wilson, S. H. (1986) *J. Biol. Chem.* **261,** 3536–3543
21. Merrill, B. M., Lopresti, M. B., Stone, K. L., and Williams, K. R. (1987) *Int. J. Pept. Protein Res.* **29,** 21–39
22. Nadler, S. G., Merrill, B. M., Roberts, W. J., Keating, K. M., Lisbin, M. J., Barnett, S. F., Wilson, S. H., and Williams, K. R. (1991) *Biochemistry* **30,** 2968–2976
23. Shamoo, Y., Abdul-Manan, N., Patten, A. M., Crawford, J. K., Pellegrini, M. C., and Williams, K. R. (1994) *Biochemistry* **33,** 8272–8281
24. Cartegni, L., Maconi, M., Morandi, E., Cobianchi, F., Riva, S., and Biamonti, G. (1996) *J. Mol. Biol.* **259,** 337–348
25. Cobianchi, F., Calvio, C., Stoppini, M., Buvoli, M., and Riva, S. (1993) *Nucleic Acids Res.* **21,** 949–955
26. Kim, S., Merrill, B. M., Rajpurohit, R., Kumar, A., Stone, K. L., Papov, V. V., Schneiders, J. M., Szer, W., Wilson, S. H., Paik, W. K., and Williams, K. R. (1997) *Biochemistry* **36,** 5185–5192
27. Abdul-Manan, N., and Williams, K. R. (1996) *Nucleic Acids Res.* **24,** 4063–4070
28. Shamoo, Y., Krueger, U., Rice, L. M., Williams, K. R., and Steitz, T. A. (1997) *Nat. Struct. Biol.* **4,** 215–222
29. Xu, R. M., Jokhan, L., Cheng, X., Mayeda, A., and Krainer, A. R. (1997) *Structure* **5,** 559–570
30. Ding, J., Hayashi, M. K., Zhang, Y., Manche, L., Krainer, A. R., and Xu, R. M. (1999) *Genes Dev.* **13,** 1102–1115
31. Parkinson, G. N., Lee, M. P., and Neidle, S. (2002) *Nature* **417,** 876–880
32. Phan, A. T., and Mergny, J. L. (2002) *Nucleic Acids Res.* **30,** 4618–4625
33. Hawkins, M. E., Pfleiderer, W., Balis, F. M., Porter, D., and Knutson, J. R. (1997) *Anal. Biochem.* **244,** 86–95
34. Hawkins, M. E. (2001) *Cell Biochem. Biophys.* **34,** 257–281
35. Otwinowski, Z., and Minor, W. (1997) *Methods Enzymol.* **276,** 307–326
36. Brunger, A. T., Adams, P. D., Clore, G. M., DeLano, W. L., Gros, P., Grosse-Kunstleve, R. W., Jiang, J.-S., Kuszewski, J., Nilges, M., Pannu, N. S., Reed, R. J., Rice, L. M., Simonson, T., and Warren, G. L. (1998) *Acta Crystallogr. Sec. D* **54,** 905–921
37. van Aalten, D. M. F. R., Bywater, R., Findlay, J. B. C., Hendlich, M., Hooft, R. W. W., and Vriend, G. (1996) *J. Comput. Aided Mol. Des.* **10,** 255–262
38. Kleywegt, G. J. (1995) *CCP4/ESF-EACBM Newsletter Protein Crystallogr.* **31,** 45–50
39. Lohman, T. M., and Bujalowski, W. (1991) *Methods Enzymol.* **208,** 258–290
40. Sun, S., and Shamoo, Y. (2003) *J. Biol. Chem.* **278,** 3876–3881
41. Zimm, B. H. (1948) *J. Chem. Phys.* **16,** 1099–1116
42. Record, M. T., Jr., Woodbury, C. P., and Lohman, T. M. (1976) *Biopolymers* **15,** 893–915
43. Mascotti, D. P., and Lohman, T. M. (1990) *Proc. Natl. Acad. Sci. U. S. A.* **87,** 3142–3146
44. Munroe, S. H., and Dong, X. F. (1992) *Proc. Natl. Acad. Sci. U. S. A.* **89,** 895–899
45. Katahira, M., Fukuda, H., Kawasumi, H., Sugimura, T., Nakagama, H., and Nagao, M. (1999) *Biochem. Biophys. Res. Commun.* **264,** 327–333
46. Allers, J., and Shamoo, Y. (2001) *J. Mol. Biol.* **311,** 75–86
47. Record, M. T., Jr., Lohman, M. L., and De Haseth, P. (1976) *J. Mol. Biol.* **107,** 145–158
48. Neidle, S., and Parkinson, G. N. (2003) *Curr. Opin. Struct. Biol.* **13,** 275–283
49. Nasim, F. U., Hutchison, S., Cordeau, M., and Chabot, B. (2002) *RNA (N. Y.)* **8,** 1078–1089
50. Carson, M. (1991) *J. Appl. Crystallogr.* **24,** 958–961